Journal of Information Systems Engineering and Management
2026, 11(3s)
e-ISSN: 2468-4376
https://www.jisem-journal.com/
Research Article

Development and Validation of a MATLAB-Based FCHEV Simulator Integrating an Equivalent Consumption Minimization Strategy for Energy Management

Lachi Brahim[1], Berkani Abderrahmane[2], Negadi Karim[3], Aouadj Norediene[4]

[123] *Department of Electrical Engineering, Faculty of Applied sciences, Universitas IBN Khaldoun of Tiaret, Algeria*

[4] *Higher School in electrical and energy engineering (ESGEE), second cycle department, Oran, Algeria*

ARTICLEINFO

Received: 11 May 2026

Revised: 01 July 2026

Accepted: 13 July 2026

ABSTRACT

Introduction: This work addresses the need for reliable simulation platforms to analyze and optimize advanced energy management strategies in sustainable transportation. It focuses on the development of a comprehensive simulation environment tailored for Fuel Cell Hybrid Electric Vehicles (FCHEV).Objectives: The primary objective is to develop and validate a robust, modular MATLAB-based simulator for an FCHEV. This includes integrating an enhanced Equivalent Consumption Minimization Strategy (ECMS) for real-time energy management while ensuring component protection and system flexibility.Methods: The simulator integrates multiphysics models of the vehicle's longitudinal dynamics, a PMSM traction motor, a lithium-ion battery, a PEM fuel cell, the transmission, a DC/DC converter, and an inverter. The ECMS algorithm is enhanced with fuel cell power gradient limitations and battery state-of-charge supervision. Validation is performed using the WLTC Class 3b driving cycle, supported by a systematic cross-validation of independent physical quantities to ensure numerical consistency and robustness.Results: The simulator successfully reproduces the complex behavior of the propulsion system. Comprehensive analysis of power flows, battery behavior, fuel cell operation, hydrogen consumption, and overall system efficiency demonstrates high accuracy, physical consistency, and numerical stability throughout the driving cycle.Conclusions: The developed MATLAB-based simulator provides a highly reliable and flexible platform. It proves to be an effective tool for the analysis, evaluation, and optimization of advanced real-time energy management strategies in fuel cell hybrid vehicles.

Keywords: Fuel Cell Hybrid Electric Vehicle (FCHEV); ECMS strategy; energy management; MATLAB simulator; WLTC cycle; PEM fuel cell; lithium-ion battery.

INTRODUCTION

The transportation sector remains one of the largest contributors to global greenhouse gas emissions and energy consumption, accounting for a significant share of worldwide CO_2 emissions. Consequently, the decarbonization of road transportation has become a strategic priority for achieving carbon neutrality and sustainable mobility [1], [2]. Electrified powertrains have therefore attracted considerable attention as an effective alternative to conventional internal combustion engine vehicles. Among them, Fuel Cell Hybrid Electric Vehicles (FCHEVs) have emerged as a promising solution because they combine zero tailpipe emissions, long driving range, fast hydrogen refueling, and high energy conversion efficiency [3], [4].

An FCHEV generally integrates a Proton Exchange Membrane Fuel Cell (PEMFC) as the primary energy source and a lithium-ion battery as an auxiliary energy storage system. The battery supplies transient power demands, absorbs regenerative braking energy, and compensates for the slow dynamic response of the fuel cell, thereby improving the overall efficiency, durability, and drivability of the vehicle [5], [6]. Although this hybrid architecture offers significant advantages over Battery Electric Vehicles (BEVs), the coexistence of two energy sources considerably increases the complexity of power management and system control.

Journal of Information Systems Engineering and Management
2026, 11(3s)
e-ISSN: 2468-4376
https://www.jisem-journal.com/

Research Article

Energy Management Strategy (EMS) has consequently become one of the most active research topics in FCHEVs. Numerous approaches have been proposed in the literature, including rule-based strategies, fuzzy logic controllers, Dynamic Programming (DP), Model Predictive Control (MPC), reinforcement learning, and Equivalent Consumption Minimization Strategy (ECMS) [2], [7], [8]. Among these methods, DP provides the theoretical global optimum but requires complete knowledge of the driving cycle, making it unsuitable for real-time implementation. Conversely, ECMS has become one of the most widely adopted real-time optimization techniques because it offers fuel economy close to the global optimum while maintaining low computational complexity [7], [9], [10].

Recent research has focused on improving the conventional ECMS by introducing adaptive equivalence factors, degradation-aware optimization, predictive control, and artificial intelligence techniques to simultaneously reduce hydrogen consumption and extend fuel cell lifetime [9]–[12]. Despite these significant advances, most published studies mainly emphasize the optimization algorithm itself, whereas comparatively few works provide a comprehensive and physically consistent simulation platform integrating detailed subsystem models, modular software architecture, rigorous numerical verification, and validation under standardized driving cycles such as the WLTC [4], [10], [13].

To address this gap, this paper presents the development and validation of a comprehensive MATLAB-based simulator for a Fuel Cell Hybrid Electric Vehicle integrating an Equivalent Consumption Minimization Strategy for real-time energy management. The proposed simulator combines multiphysics models of the vehicle longitudinal dynamics, Permanent Magnet Synchronous Motor (PMSM), lithium-ion battery, PEM fuel cell, transmission system, DC/DC converter, and inverter within a modular software framework. Furthermore, the conventional ECMS algorithm is enhanced by incorporating fuel cell power gradient limitation and battery state-of-charge supervisory constraints to improve operational realism and component protection. The simulator is evaluated using the WLTC Class 3b driving cycle through detailed analyses of vehicle dynamics, power flows, hydrogen consumption, battery behavior, and overall energy efficiency. The obtained results demonstrate the numerical robustness, physical consistency, and effectiveness of the proposed simulation platform for the analysis and optimization of advanced FCHEV energy management strategies.

ARCHITECTURE DU VEHICULE FCHEV ET MODELISATION DU SYSTEME

Architecture generale du fchev

Our fuel cell hybrid electric vehicle (FCHEV) combines two energy sources of fundamentally different natures: a fuel cell, which produces electricity from hydrogen stored on board, and a battery, which stores and delivers electrical energy [14]. This dual-source architecture makes it possible to combine the complementary qualities of the two components — the fuel cell's high energy density, offset by its limited power density and slow response dynamics [15], versus the battery's high power density but lower energy density [16] — but it raises in return a central question: how should the power demanded by the driver be split, at every instant, between these two sources so as to minimize hydrogen consumption while keeping the battery's state of charge within a safe operating range [17]? This is precisely the question addressed by the Equivalent Consumption Minimization Strategy (ECMS), adopted in this work for its well-established trade-off between energy performance and suitability for real-time implementation [18].

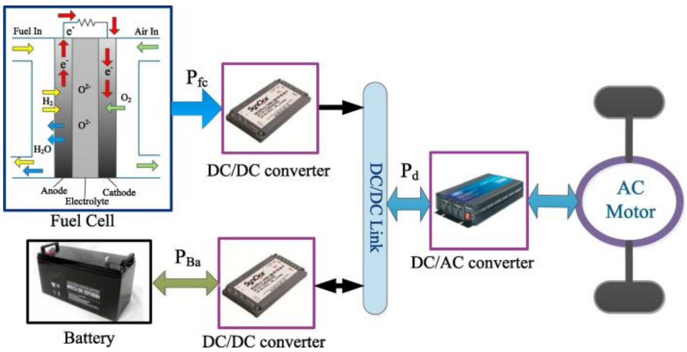

Figure 1: Architecture of the studied vehicle

Journal of Information Systems Engineering and Management
2026, 11(3s)
e-ISSN: 2468-4376
https://www.jisem-journal.com/

Research Article

VEHICLE DYNAMIC MODEL

Modeling of the FCHEV Vehicle Energy Traction Chain

Vehicle Dynamic Model

The fundamental principle of longitudinal dynamics is based on the application of Newton's second law. The general equation of longitudinal dynamics is then written as [19] [20]:

$$F_{tr} = F_{roll} + F_{aero} + F_{grade} + F_{acc} \tag{1}$$

The rolling resistance is then expressed as:

$$F_{roll} = C_{rr}\, m\, g \tag{2}$$

Aerodynamic resistance, also known as aerodynamic drag force, corresponds to the force exerted by the air on the vehicle as it moves. It is expressed as:

$$F_{aero} = \frac{1}{2}\rho C_d A_f v^2 \tag{3}$$

The resistance due to the grade is therefore written as:

$$F_{grade} = mg\sin\theta \tag{4}$$

By applying Newton's second law to the longitudinal motion of the vehicle, the inertial force is given by:

$$F_{acc} = m\, a \tag{5}$$

Acceleration is obtained from the time derivative of the velocity:

$$a = \frac{dv}{dt} \tag{6}$$

PMSM Motor Model

In the d–q rotating reference frame, the electrical equations of the PMSM motor are written as |21]-[23]:

$$v_d = R_s i_d + \frac{d\lambda_d}{dt} - \omega_e \lambda_q \tag{7}$$

$$v_q = R_s i_q + \frac{d\lambda_q}{dt} + \omega_e \lambda_d \tag{8}$$

The magnetic flux linkages are given by:

$$\lambda_d = L_d i_d + \lambda_f \tag{9}$$

$$\lambda_q = L_q i_q \tag{10}$$

The general expression of the electromagnetic torque of a PMSM:

$$T_e = \frac{3}{2} p\left(\lambda_d i_q - \lambda_q i_d\right) \tag{11}$$

The mechanical behavior of the rotor is governed by the fundamental principle of dynamics applied to rotational motion.

$$T_e - T_L - T_f = J\frac{d\omega_m}{dt} \tag{12}$$

Li-Ion Battery Model

The model adopted represents the battery as an ideal voltage source, corresponding to the battery's open-circuit voltage, placed in series with an internal resistance.

The open-circuit voltage, denoted, can be expressed as a function of the SOC:

$$V_{oc} = V_{min} + (V_{max} - V_{min})SOC \tag{13}$$

In this work, the internal resistance is considered constant, which is a reasonable assumption for the energy simulations carried out.

Journal of Information Systems Engineering and Management
2026, 11(3s)
e-ISSN: 2468-4376
https://www.jisem-journal.com/ **Research Article**

$$\boxed{R_{int} = R_0} \quad (14) \tag{14}$$

By applying Kirchhoff's voltage law, the voltage across the battery terminals is written as:

During discharge:

$$\boxed{V_{bat} = V_{oc} - R_{int} I_{bat}} \tag{15}$$

During charge:

$$\boxed{V_{bat} = V_{oc} + R_{int} I_{bat}} \tag{16}$$

This equivalent model is commonly used in FCHEV and hybrid electric vehicle studies for system-level energy management analysis and control design [24]–[27].

PEM Fuel Cell Model

The actual voltage of a PEMFC cell is obtained by subtracting all the losses from the reversible voltage. The general expression is written as:

$$\boxed{V_{cell} = E_N - \eta_{act} - \eta_{ohm} - \eta_{conc}} \tag{17}$$

This relation constitutes the fundamental electrochemical model of the PEMFC cell.

The concentration overvoltage is defined as:

$$\eta_{conc} = -\frac{RT}{2F} \ln\left(1 - \frac{I}{I_L}\right) \tag{18}$$

The stack voltage is obtained by:

$$\boxed{V_{stack} = N_{cell} V_{cell}} \tag{19}$$

Substituting V_{cell} with equation (2.220), we obtain:

$$\boxed{V_{stack} = N_{cell}(E_N - \eta_{act} - \eta_{ohm} - \eta_{conc})} \tag{20}$$

The instantaneous power produced by the stack is given by:

$$\boxed{P_{FC} = V_{stack} I_{FC}} \tag{21}$$

The molar flow rate of hydrogen consumed is directly related to the current supplied by the stack:

$$\boxed{\dot{n}_{H_2} = \frac{I_{FC}}{2F}} \tag{22}$$

The mass flow rate of hydrogen is calculated by:

$$\boxed{\dot{m}_{H_2} = M_{H_2} \frac{I_{FC}}{2F}} \tag{23}$$

$$M_{H_2} = 2.016 \times 10^{-3} \text{ kg mol}^{-1}$$

The total mass flow rate becomes:

$$\boxed{\dot{m}_{H_2} = N_{cell} M_{H_2} \frac{I_{FC}}{2F}} \tag{24}$$

The total mass of hydrogen consumed over an operating period is obtained by integrating the mass flow rate:

$$\boxed{m_{H_2} = \int_0^t \dot{m}_{H_2}(\tau)\, d\tau} \tag{25}$$

To compare different propulsion systems, it is useful to define the specific hydrogen consumption. It is written as:

$$\boxed{C_{sp} = \frac{\dot{m}_{H_2}}{P_{FC}}} \tag{26}$$

For fuel cell vehicles, the lower heating value of hydrogen (LHV) is generally used, since the water produced leaves the cell mainly in vapor form. Its value is:

$$\boxed{PCI_{H_2} = 120 \times 10^6 \text{ J kg}^{-1}} \tag{27}$$

The instantaneous efficiency of the fuel cell is written as:

Journal of Information Systems Engineering and Management
2026, 11(3s)
e-ISSN: 2468-4376
https://www.jisem-journal.com/

Research Article

$$\eta_{FC} = \frac{P_{FC}}{\dot{m}_{H_2} PCI_{H_2}} \tag{28}$$

This electrochemical model is widely used in FCHEV system-level simulations due to its good compromise between physical accuracy and computational tractability [28]–[31].

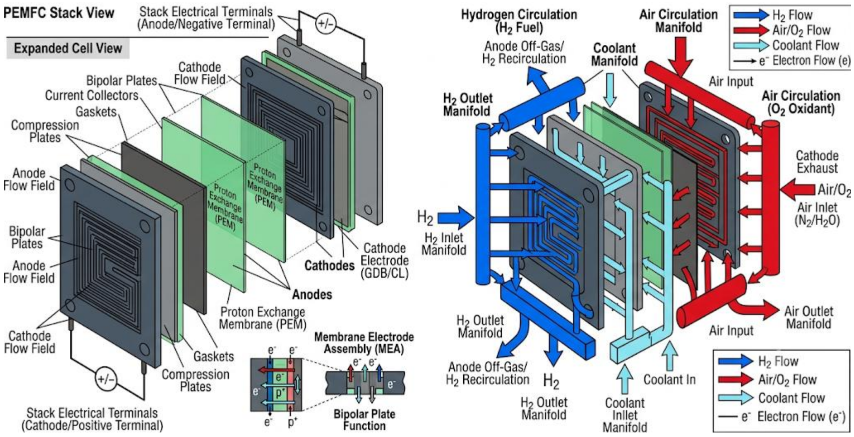

Figure 2. General architecture of a PEMFC stack.

Modeling of the Bidirectional DC/DC Converter

The state variables that fully describe the dynamics of the converter are therefore [32], [33]:

$$x = \begin{bmatrix} i_L \\ V_{dc} \end{bmatrix} \tag{29}$$

$$v_L = L\frac{di_L}{dt} \tag{30}$$

$$i_C = C\frac{dV_{dc}}{dt} \tag{31}$$

Boost Mode Operation

By applying Kirchhoff's laws, the following average equations are obtained.

$$L\frac{di_L}{dt} = V_{FC} - (1 - D)V_{dc} \tag{32}$$

$$C\frac{dV_{dc}}{dt} = (1 - D)i_L - i_{load} \tag{33}$$

Buck Mode Operation

Equations (2.244) and (2.245) fully describe the dynamics of the converter in Boost mode.

$$L\frac{di_L}{dt} = DV_{dc} - V_{bat} \tag{34}$$

$$C\frac{dV_{dc}}{dt} = i_{FC} - Di_L - i_{load} \tag{35}$$

Averaged State-Space Model

In order to have a single model valid regardless of the operating mode, the previous equations are combined into the form of a state-space model:

$$\dot{x} = Ax + Bu \tag{36}$$

With :

$$x = \begin{bmatrix} i_L \\ V_{dc} \end{bmatrix}$$

and

Journal of Information Systems Engineering and Management
2026, 11(3s)
e-ISSN: 2468-4376
https://www.jisem-journal.com/ **Research Article**

$$u = \begin{bmatrix} V_{FC} \\ V_{bat} \\ i_{load} \end{bmatrix} \quad (37)$$

The matrices A and B depend on the duty cycle and the parameters and. They are recalculated at each simulation step according to the operating mode.

The fundamental parameter of the converter is the duty cycle:

$$D = \frac{t_{on}}{T_s} \quad (38)$$

In steady-state ideal operation, the relationship between the voltages depends on the operating mode.

Boost Mode

$$V_{dc} = \frac{V_{FC}}{1-D} \quad (39)$$

Buck Mode

$$V_{bat} = DV_{dc} \quad (40)$$

The total power dissipated in the converter can be expressed as:

$$P_{loss} = P_{cond} + P_{sw} + P_{mag} + P_{aux} \quad (41)$$

For system-level simulations, the last two terms are often neglected when they remain small compared to the main losses.

Converter Efficiency

The instantaneous efficiency of the converter is defined as follows:

$$\eta_{DC/DC} = 1 - \frac{P_{loss}}{P_{in}} \quad (42)$$

Depending on the direction of energy transfer, the following relations are used.

Boost Mode Operation

$$P_{dc} = \eta_{DC/DC} P_{FC} \quad (43)$$

Buck Mode Operation

$$P_{bat} = \eta_{DC/DC} P_{dc} \quad (44)$$

Modern DC/DC converters intended for hybrid vehicles generally exhibit an efficiency between:

$$95\% \le \eta_{DC/DC} \le 98.5\% \quad (45)$$

THE PROPOSED ECMS STRATEGY

Objectives and Constraints of Energy Management

The main objective adopted in this paper is the minimization of hydrogen consumption while ensuring compliance with the vehicle's dynamic performance [34]-[36].

The fundamental power balance constraint is written as:

$$P_{dem} = P_{FC} + P_{bat} \quad (46)$$

In addition to reducing hydrogen consumption, several secondary objectives must be satisfied.

a) Maintaining the battery state of charge

The battery must operate within a charge range compatible with the manufacturer's recommendations in order to preserve its lifespan. This constraint is written as:

Journal of Information Systems Engineering and Management
2026, 11(3s)
e-ISSN: 2468-4376
https://www.jisem-journal.com/
Research Article

$$SOC_{min} \leq SOC \leq SOC_{max} \tag{47}$$

b) Optimal fuel cell operation

To improve the overall efficiency of the system, it is desirable to keep the fuel cell within its zone of maximum efficiency. The delivered power must therefore satisfy:

$$P_{FC}^{min} \leq P_{FC} \leq P_{FC}^{max} \tag{48}$$

c) Compliance with battery limits

The battery also has operating limits in charge and discharge:

$$P_{bat}^{min} \leq P_{bat} \leq P_{bat}^{max} \tag{49}$$

The voltages and currents of the various components must remain within their operating ranges. For the fuel cell:

$$V_{FC}^{min} \leq V_{FC} \leq V_{FC}^{max} \tag{50}$$

and

$$I_{FC}^{min} \leq I_{FC} \leq I_{FC}^{max} \tag{51}$$

The fuel cell cannot change its power instantaneously. The power variation is therefore limited by:

$$\left| \frac{dP_{FC}}{dt} \right| \leq R_{FC} \tag{52}$$

where R_{FC} represents the maximum admissible power ramp rate.

The evolution of the state of charge is given by:

$$\frac{dSOC}{dt} = -\frac{I_{bat}}{Q_{nom}} \tag{53}$$

In the ECMS strategy, the decision variables are the power exchanged between the two sources. The decision vector is defined by:

$$u = \begin{bmatrix} P_{FC} \\ P_{bat} \end{bmatrix} \tag{54}$$

Given the power balance (2.263), only one of these variables is independent. In practice, ECMS generally chooses P_{FC}, while the battery power is obtained by:

$$P_{bat} = P_{dem} - P_{FC} \tag{55}$$

The above objectives and constraints lead to the following instantaneous optimization problem:

$$\min_{P_{FC}} J \tag{56}$$

subject to the constraints:

$$\begin{cases} P_{dem} = P_{FC} + P_{bat} \\ SOC_{min} \leq SOC \leq SOC_{max} \\ P_{FC}^{min} \leq P_{FC} \leq P_{FC}^{max} \\ P_{bat}^{min} \leq P_{bat} \leq P_{bat}^{max} \\ \left| \frac{dP_{FC}}{dt} \right| \leq R_{FC} \end{cases} \tag{57}$$

The total equivalent consumption is defined as the sum:

$$\dot{m}_{eq} = \dot{m}_{H_2} + \dot{m}_{bat}^{eq} \tag{58}$$

The objective of ECMS is to determine the fuel cell power that minimizes the instantaneous equivalent consumption. The optimization problem is written as:

$$P_{FC}^{*} = \arg\min_{P_{FC}} \left(\dot{m}_{eq}\right) \tag{59}$$

Expanding the above expression, we obtain:

Journal of Information Systems Engineering and Management
2026, 11(3s)
e-ISSN: 2468-4376
https://www.jisem-journal.com/
Research Article

$$P_{FC}^{*} = \arg\min_{P_{FC}}\left(\dot{m}_{H_2} + \dot{m}_{bat}^{eq}\right) \tag{60}$$

This relation constitutes the fundamental principle of ECMS.

The power demand imposed by the driver is split between the two sources according to:

$$P_{dem} = P_{FC} + P_{bat} \tag{61}$$

The battery power is therefore:

$$P_{bat} = P_{dem} - P_{FC} \tag{62}$$

The optimization problem thus involves only a single decision variable, namely the power delivered by the fuel cell.

The fuel cell power must satisfy the physical constraints of the system:

$$P_{FC}^{min} \le P_{FC} \le P_{FC}^{max} \tag{63}$$

The mass flow rate of hydrogen consumed by the fuel cell is directly related to the electric power produced. Using the relations established in Section 2.6, we can write:

$$\dot{m}_{H_2} = \frac{P_{FC}}{\eta_{FC}\, PCI_{H_2}} \tag{64}$$

The battery power is defined by:

$$P_{bat} = V_{bat} I_{bat} \tag{65}$$

with the following convention:

$$\begin{cases} P_{bat} > 0 & \text{battery discharging} \\ P_{bat} < 0 & \text{battery charging} \end{cases} \tag{66}$$

The energy supplied or absorbed by the battery is converted into an equivalent hydrogen consumption using the equivalence factor s. The equivalent consumption is given by:

$$\dot{m}_{bat}^{eq} = s\,\frac{P_{bat}}{PCI_{H_2}} \tag{67}$$

The energy efficiency of the battery differs depending on the direction of power exchange. In discharge mode:

$$\dot{m}_{bat}^{eq} = s\,\frac{P_{bat}}{\eta_{dis}\, PCI_{H_2}} \tag{68}$$

$$\dot{m}_{bat}^{eq} = s\,\frac{\eta_{ch} P_{bat}}{PCI_{H_2}} \tag{69}$$

The instantaneous cost function is obtained by adding the actual fuel cell consumption and the equivalent battery consumption. It is written as:

$$J = \dot{m}_{H_2} + \dot{m}_{bat}^{eq} \tag{70}$$

Substituting the previous expressions:

$$J = \frac{P_{FC}}{\eta_{FC} PCI_{H_2}} + s\,\frac{P_{bat}}{\eta_{bat} PCI_{H_2}} \tag{71}$$

where η_{bat} represents the appropriate efficiency (charging or discharging).

This equation constitutes the fundamental cost function used by ECMS.

The cost function then depends only on the power supplied by the fuel cell:

$$J(P_{FC}) = \frac{P_{FC}}{\eta_{FC} PCI_{H_2}} + s\,\frac{P_{dem} - P_{FC}}{\eta_{bat} PCI_{H_2}} \tag{72}$$

This expression constitutes the function actually minimized in the simulator.

ECMS seeks the fuel cell power that minimizes the cost function:

$$P_{FC}^{*} = \arg\min_{P_{FC}} J(P_{FC}) \tag{73}$$

subject to the constraints:

Journal of Information Systems Engineering and Management
2026, 11(3s)
e-ISSN: 2468-4376
https://www.jisem-journal.com/

Research Article

$$P_{FC}^{min} \leq P_{FC} \leq P_{FC}^{max} \quad (74)$$

and

$$SOC_{min} \leq SOC \leq SOC_{max} \quad (75)$$

DEVELOPMENT OF THE MATLAB SIMULATOR

The main objective of the simulator is to provide a numerical platform capable of reproducing the energy behavior of a fuel cell hybrid electric vehicle operating on a standardized driving cycle.

Software Architecture of the Simulator

The simulator is based on a modular, functional software architecture rather than an object-oriented one: each physical subsystem (vehicle, motor, battery, fuel cell, energy management strategy) is implemented as an independent MATLAB function, taking parameter structures as input and returning a results structure.

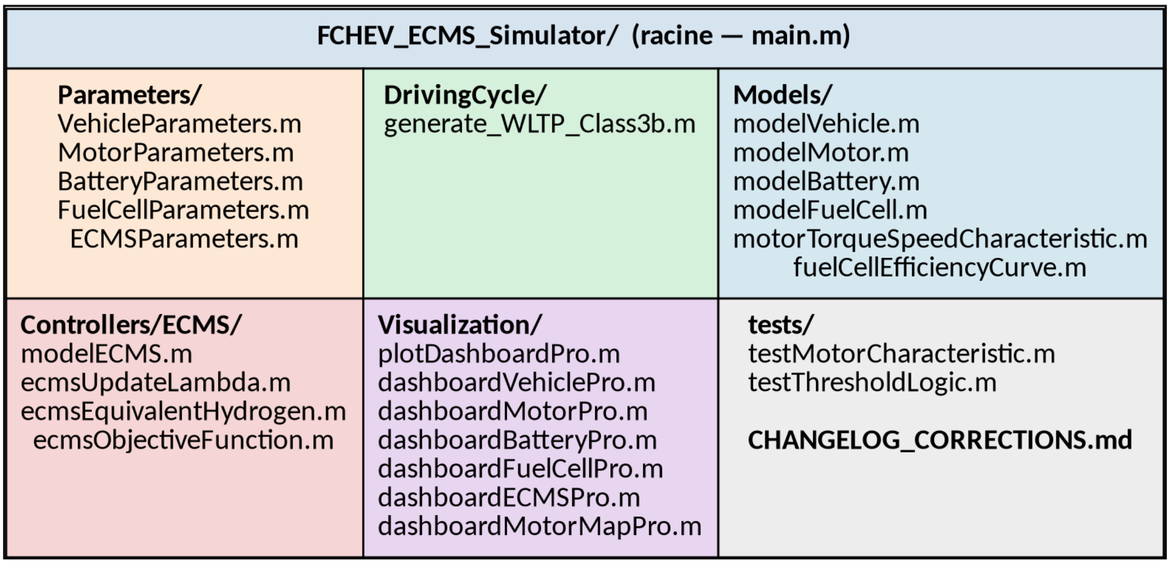

Figure 3: Folder and file structure of the FCHEV_ECMS_Simulator

The computation flow of the simulator follows a strictly sequential chain, with each module consuming the results of the previous one in the form of MATLAB structures. This sequence, orchestrated by main.m, is broken down as follows:

- Parameter loading — the five functions in the Parameters/ folder are called to build the Vehicle, Motor, Battery, FuelCell, and ECMS structures.
- Driving cycle generation — generate_WLTP_Class3b() produces the Cycle structure (time, speed, distance, phases).
- Vehicle model — modelVehicle(Cycle, Vehicle) computes the longitudinal kinematics and dynamics (acceleration, traction force, wheel torque, required motor power).
- Motor model — modelMotor(VehicleModel, Motor, Vehicle) converts this demand into motor torque and speed, and computes the corresponding electric power.
- ECMS model — modelECMS(MotorModel, Battery, FuelCell, ECMS, Cycle) determines, at each time step, the optimal power split between the fuel cell and the battery, itself tracking the evolution of the SOC internally.
- Detailed battery and fuel cell models — modelBattery() and modelFuelCell() each receive, as input, the power profile decided by the ECMS (rather than the vehicle's total demand), and derive the detailed electrical quantities from it (voltage, current, losses, hydrogen consumption).

Journal of Information Systems Engineering and Management
2026, 11(3s)
e-ISSN: 2468-4376
https://www.jisem-journal.com/ **Research Article**

- Visualization — plotDashboardPro() assembles all the results into five dashboards and a complete characterization of the motor.

Table 1: Vehicle parameters

Parameter	Symbol / field	Value	Unit
Vehicle mass	Vehicle.mass	1662	kg
Wheel radius	Vehicle.wheelRadius	0.294	m
Transmission efficiency	Vehicle.transmissionEfficiency	0.98	—
Rolling resistance coefficient	Vehicle.Cr	0.01	—
Aerodynamic drag coefficient	Vehicle.Cd	0.25	—
Frontal area	Vehicle.frontalArea	2.04	m^2
Maximum motor power (reference vehicle)	Vehicle.motorMaxPower	75 000	W
Maximum motor speed (reference vehicle)	Vehicle.motorMaxSpeed	1256.6	rad/s
Maximum regeneration power	Vehicle.maxRegenPower	-30 000	W
Gravity	Vehicle.g	9.81	m/s^2
Air density	Vehicle.rhoAir	1.225	kg/m^3

Table 2: Electric motor parameters (PMSM)

Parameter	Field	Value	Unit
Rated power	Motor.nominalPower	40 000	W
Maximum power	Motor.maxPower	75 000	W
Maximum torque	Motor.maxTorque	220	N.m
Continuous rated torque	Motor.nominalTorque	130	N.m
Base speed	Motor.baseSpeedRPM	3000	tr/min
Maximum speed	Motor.maxSpeedRPM	12 000	tr/min
Rated efficiency	Motor.nominalEfficiency	0.95	—
Minimum efficiency	Motor.minimumEfficiency	0.82	—
Maximum efficiency	Motor.maximumEfficiency	0.96	—
Inertia	Motor.inertia	0.015	$kg.m^2$

Journal of Information Systems Engineering and Management
2026, 11(3s)
e-ISSN: 2468-4376
https://www.jisem-journal.com/
Research Article

Gear ratio	Motor.gearRatio	9	—
Auxiliary losses (cooling)	Motor.coolingLoss	300	W
Maximum current	Motor.maximumCurrent	300	A
Maximum voltage	Motor.maximumVoltage	400	V
Regeneration efficiency	Motor.regenerationEfficiency	0.90	—

Table 3: Li-Ion battery parameters

Parameter	Field	Value	Unit
Nominal voltage	Battery.nominalVoltage	360	V
Capacity	Battery.capacity	25	Ah
Nominal energy	Battery.nominalEnergy	9000	Wh
Initial SOC	Battery.initialSOC	0.65 (65%)	—
Minimum SOC	Battery.minimumSOC	0.20 (20%)	—
Maximum SOC	Battery.maximumSOC	0.90 (90%)	—
Charge efficiency	Battery.chargeEfficiency	0.95	—
Discharge efficiency	Battery.dischargeEfficiency	0.95	—
Internal resistance	Battery.internalResistance	0.08	Ω
Maximum discharge power	Battery.maximumDischargePower	50 000	W
Maximum charge power	Battery.maximumChargePower	-35 000	W

Table 4: Fuel cell PEM parameters

Parameter	Field	Value	Unit
Rated power	FuelCell.nominalPower	50 000	W
Maximum power	FuelCell.maximumPower	60 000	W
Minimum power	FuelCell.minimumPower	0	W
Nominal voltage (stack)	FuelCell.nominalVoltage	300	V
Number of cells	FuelCell.numberOfCells	350	—
Rated efficiency	FuelCell.nominalEfficiency	0.55	—
Maximum efficiency	FuelCell.maximumEfficiency	0.60	—
Minimum efficiency	FuelCell.minimumEfficiency	0.40	—

Journal of Information Systems Engineering and Management
2026, 11(3s)
e-ISSN: 2468-4376
https://www.jisem-journal.com/ **Research Article**

Lower heating value (H2)	FuelCell.lowerHeatingValue	120.10^6	J/kg
Time constant	FuelCell.timeConstant	2.0	s
Maximum power gradient	FuelCell.rampRate	10 000	W/s
DC/DC converter efficiency	FuelCell.converterEfficiency	0.97	—
Auxiliary power	FuelCell.auxiliaryPower	500	W

Table 5: ECMS strategy parameters

Parameter	Field	Value	Unit
Sampling time	ECMS.sampleTime	1	s
Initial equivalence factor	ECMS.lambda0	2.5	—
Minimum equivalence factor	ECMS.minimumLambda	1.5	—
Maximum equivalence factor	ECMS.maximumLambda	4.0	—
Adaptation gain of λ	ECMS.lambdaGain	8	—
Reference SOC	ECMS.referenceSOC	0.60 (60%)	—
High SOC threshold (electric mode)	ECMS.socHighThreshold	0.80 (80%)	—
Low SOC threshold (active recharge)	ECMS.socLowThreshold	0.40 (40%)	—
Power threshold in all-electric mode	ECMS.pureElectricPowerThreshold	10 000	W
Active recharge power boost	ECMS.chargeBoostPower	8 000	W

Figure 4 summarizes, in the form of a flowchart, the complete sequence of computation steps, from parameter loading through to the production of the visual results.

Implementation of ECMS strategy

This section presents the implementation of the ECMS-based energy management algorithm, including its mathematical formulation and operating constraints. Its performance is evaluated through simulations conducted on the WLTC Class 3b driving cycle.

Principle of ECMS

The Equivalent Consumption Minimization Strategy (ECMS) is a real-time energy management approach that optimally distributes the power demand between the fuel cell and the battery by minimizing an equivalent hydrogen consumption. Based on the equivalence between battery energy and future hydrogen consumption, ECMS

Journal of Information Systems Engineering and Management
2026, 11(3s)
e-ISSN: 2468-4376
https://www.jisem-journal.com/ **Research Article**

converts electrical energy into an equivalent fuel cost, enabling instantaneous optimization. Unlike Dynamic Programming, ECMS achieves near-optimal energy efficiency with low computational complexity, making it well suited for real-time FCHEV applications.

Fonction coût

ECMS Instantaneous Cost Function

At each time step, ECMS minimizes an instantaneous cost function ($J(t)$), defined as the sum of the fuel cell hydrogen consumption and the battery equivalent hydrogen consumption weighted by the equivalence factor ($\lambda(t)$)):

$$\boxed{J(t) = \dot{m}_{H_2,real}\big(P_{FC}(t)\big) + \lambda(t)\dot{m}_{H_2,eq}\big(P_{bat}(t)\big)} \quad (76)$$

The fuel cell hydrogen consumption is derived from its output power and instantaneous efficiency as:

$$\boxed{\dot{m}_{H_2,real} = \frac{P_{FC}}{\eta_{FC}(P_{FC}).PCI}} \quad (77)$$

The battery equivalent hydrogen consumption is computed using a reference fuel cell efficiency:

$$\boxed{\dot{m}_{H_2,eq} = \frac{|P_{bat}|}{\eta_{bat}.\eta_{FC,ref}.PCI}} \quad (78)$$

where ($\eta_{FC,ref} = 0.55$) is a fixed nominal efficiency used as a common conversion basis to ensure a consistent comparison between the two energy sources.

This cost function is evaluated for each candidate fuel cell power at every time step, and the optimal operating point is selected as the one minimizing ($J(t)$), ensuring real-time optimal power split between the fuel cell and the battery.

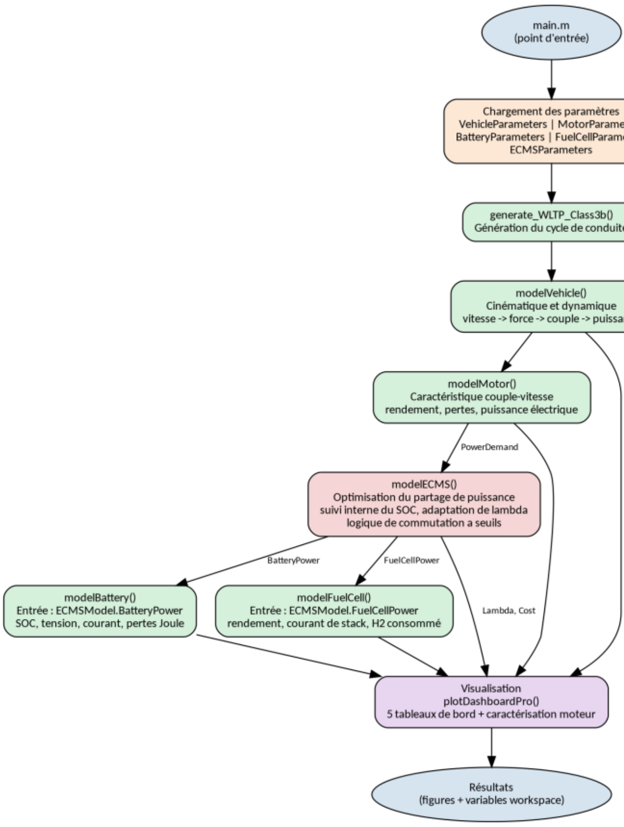

Figure 4 : General flowchart of the FCHEV_ECMS_Simulator.

Journal of Information Systems Engineering and Management
2026, 11(3s)
e-ISSN: 2468-4376
https://www.jisem-journal.com/
Research Article

Equivalence Factor λ

The equivalence factor λ represents an energy pricing parameter that converts battery electrical energy into an equivalent hydrogen cost, thus governing the power split between the fuel cell and the battery. It increases the penalty on battery usage when high and favors battery operation when low, and corresponds theoretically to the costate variable of the SOC in the Pontryagin minimum principle formulation of ECMS.

In this simulator, λ is updated at each time step using a linear SOC feedback law and is constrained within predefined limits to ensure stability and physical consistency.

$$\boxed{\lambda(k) = \lambda_0 + k(SOC_{ref} - SOC(k))} \quad (79)$$

Table 6: ECMS Equivalence Factor Parameters

Parameter	**Champ**	**Valeur**
Initial value	ECMS.lambda0	2,5
Initial value Reference SOC	ECMS.referenceSOC	0,60 (60 %)
Adaptation gain	ECMS.lambdaGain (K)	8
Lower bound	ECMS.minimumLambda	1,5
Upper bound	ECMS.maximumLambda	4,0

Constraints

The decision algorithm explores, at each time step, a set of fuel cell power candidates, filtered by three families of physical constraints before their cost is evaluated.

The SOC constraint is checked predictively: for each candidate, the resulting SOC at the next time step is computed using coulomb counting (the same formula as in modelBattery.m) before the candidate is accepted or rejected, ensuring that no decision can push the SOC outside its admissible range.

Table 7: Battery Constraints

Contraint	**Expression**	**Role**
Maximum discharge power	P_bate ≤ PmaxDischarge = 50 kW	Physical limit of the pack
Maximum charge power	P_bat ≥ PmaxCharge = -35 kW	Physical limit of the pack
Minimum SOC	SOC(k+1) ≥ SOCmin = 20 %	Protection against deep discharge
Maximum SOC	SOC(k+1) ≤ SOCmax = 90 %	Protection against overcharge

Table 8: Fuel Cell Constraints

Contraint	**Expression**	**Role**
Minimum power	P_pile ≥ PfcMin = 0 kW	The fuel cell cannot absorb power
Minimum power	P_pile ≤ PfcMax = 60 kW	Physical limit of the stack

Journal of Information Systems Engineering and Management
2026, 11(3s)
e-ISSN: 2468-4376
https://www.jisem-journal.com/

Research Article

Power gradient	|P_pile(k) – P_pile(k–1)| ≤ rampRate · Δt = 10 kW	Physical inertia

The fuel cell cannot absorb power Physical limit of the stack Physical inertia

Decision Algorithm

The algorithm, implemented in modelECMS.m, proceeds by exhaustive discrete search over a grid of fuel cell power candidates, at each time step of the cycle. Its execution is summarized by the flowchart in Figure 4.3, and can be outlined by the following pseudo-code:

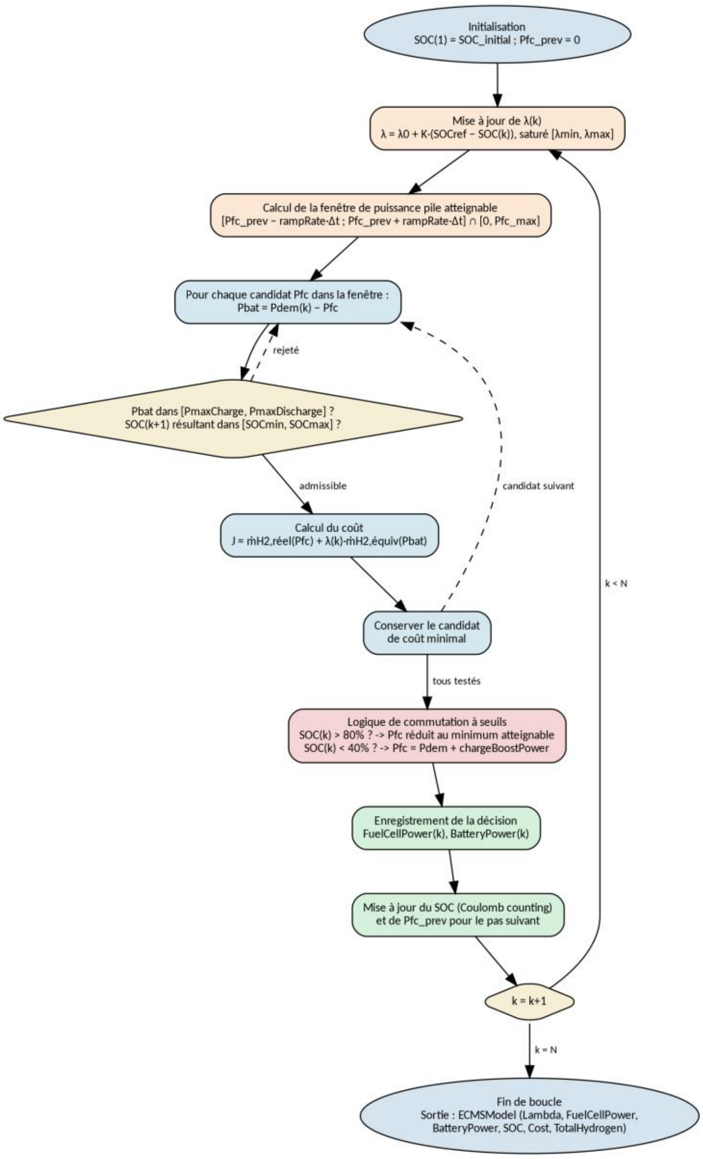

Figure 5: Flowchart of the ECMS Decision Algorithm

SIMULATION RESULTS AND DISCUSSION

This section presents and discusses the simulation results obtained using the FCHEV_ECMS_Simulator developed in MATLAB, under the official WLTC Class 3b driving cycle (1800 s, 23.27 km). The simulated vehicle is a Fuel Cell Hybrid Electric Vehicle (FCHEV), whose propulsion system combines a Proton Exchange Membrane Fuel Cell (PEMFC) and a lithium-ion (Li-ion) battery, coordinated by an Equivalent Consumption Minimization Strategy

Journal of Information Systems Engineering and Management
2026, 11(3s)
e-ISSN: 2468-4376
https://www.jisem-journal.com/ **Research Article**

(ECMS) for real-time energy management. The results are organized into six commented figures (Figures 6–12), followed by an overall discussion (Section 5.8) and a validation appendix.

Analysis of the WLTC Class 3b Driving Cycle

Figure 6 illustrates the WLTC Class 3b driving cycle adopted as the input profile for the developed FCHEV simulator. As the current international standard for light-duty vehicle certification, it combines urban, suburban, rural, and highway driving conditions within a single cycle, generating highly dynamic speed and power demand profiles. The resulting variations in traction requirements effectively challenge the energy management system under realistic operating conditions, including rapid accelerations, decelerations, cruising phases, and regenerative braking events. Consequently, the WLTC Class 3b cycle provides a representative benchmark for assessing the proposed ECMS in terms of power-sharing capability, hydrogen consumption, regenerative energy recovery, and battery state-of-charge regulation under diverse driving scenarios.

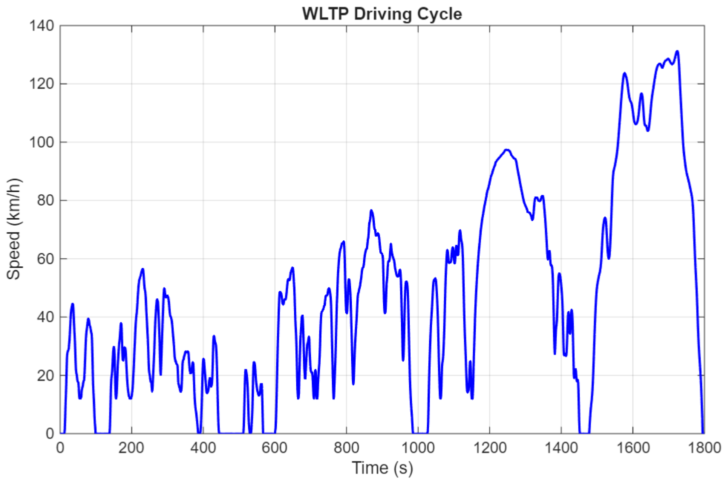

Figure 6: WLTC Driving Cycle

Vehicle Dynamics

Figure 7 presents the complete dynamic response of the vehicle over the WLTC Class 3b driving cycle by illustrating the evolution of vehicle speed, longitudinal acceleration, traction force, wheel torque, and motor power throughout the 1800 s simulation. It establishes the link between the prescribed driving cycle and the power demand delivered to the electric powertrain. The mechanical quantities are computed using the vehicle longitudinal dynamics model, which accounts for inertial effects, rolling resistance, and aerodynamic drag.

As shown in Figure 7, variations in the speed profile produce significant fluctuations in traction force, wheel torque, and the power required from the electric motor. During acceleration phases, the inertial component dominates the longitudinal dynamics, resulting in power peaks of approximately 45 kW. In contrast, deceleration phases are characterized by negative motor power, indicating generator operation and energy recovery through regenerative braking. At higher vehicle speeds, aerodynamic drag becomes the dominant resistive force, substantially increasing the propulsion power required to maintain vehicle speed, particularly during the Extra High phase of the WLTC driving cycle.

Therefore, Figure 7 highlights the highly dynamic nature of the power demand imposed on the propulsion system and provides a fundamental basis for evaluating the proposed Equivalent Consumption Minimization Strategy (ECMS). The resulting power profile constitutes the primary input to the energy management controller, which must optimally allocate power between the proton exchange membrane fuel cell (PEMFC) and the lithium-ion battery in real time while maximizing regenerative energy recovery and minimizing hydrogen consumption. These results also confirm the consistency of the developed vehicle dynamic model, from vehicle kinematics to the estimation of the power demand supplied to the electric drivetrain.

Journal of Information Systems Engineering and Management
2026, 11(3s)
e-ISSN: 2468-4376
https://www.jisem-journal.com/

Research Article

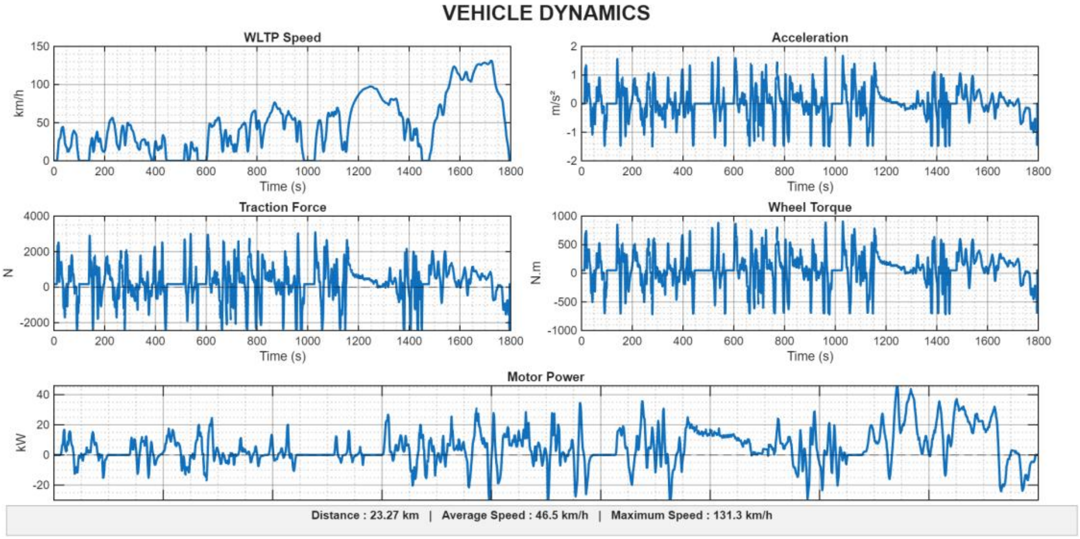

Figure 7: Dynamic response of the vehicle over the WLTC Class 3b

Electric Motor

Figure 8 illustrates the electromechanical behavior of the Permanent Magnet Synchronous Motor (PMSM) throughout the WLTC Class 3b driving cycle by presenting the evolution of motor speed, electromagnetic torque, mechanical power, instantaneous efficiency, and motor losses. The motor operates according to a conventional two-region torque–speed characteristic, consisting of a constant-torque region followed by a constant-power region, as defined in the developed electric powertrain model.

The results demonstrate excellent consistency between the motor response and the vehicle dynamics. The maximum motor torque (approximately 102.8 N·m), combined with the transmission gear ratio, produces a wheel torque that agrees with the value obtained from the previous dynamic analysis, thereby validating the implemented electromechanical model. The instantaneous motor efficiency remains predominantly within the 90–96% range, indicating operation in a highly efficient region. The lower average efficiency observed over the complete driving cycle is mainly attributed to the numerous low-load operating conditions encountered during vehicle stops and urban driving, where fixed losses become proportionally more significant.

Furthermore, Figure 8 shows that the PMSM operates entirely within its nominal operating envelope, without approaching its torque or speed limits throughout the WLTC cycle. The electrical power required by the motor constitutes one of the primary inputs to the Equivalent Consumption Minimization Strategy (ECMS), while the conversion losses indirectly affect the power distribution between the proton exchange membrane fuel cell (PEMFC) and the lithium-ion battery. These findings confirm the adequacy of the motor sizing and demonstrate its capability to satisfy the dynamic requirements imposed by the WLTC driving cycle while maintaining a high level of energy efficiency.

Journal of Information Systems Engineering and Management
2026, 11(3s)
e-ISSN: 2468-4376
https://www.jisem-journal.com/

Research Article

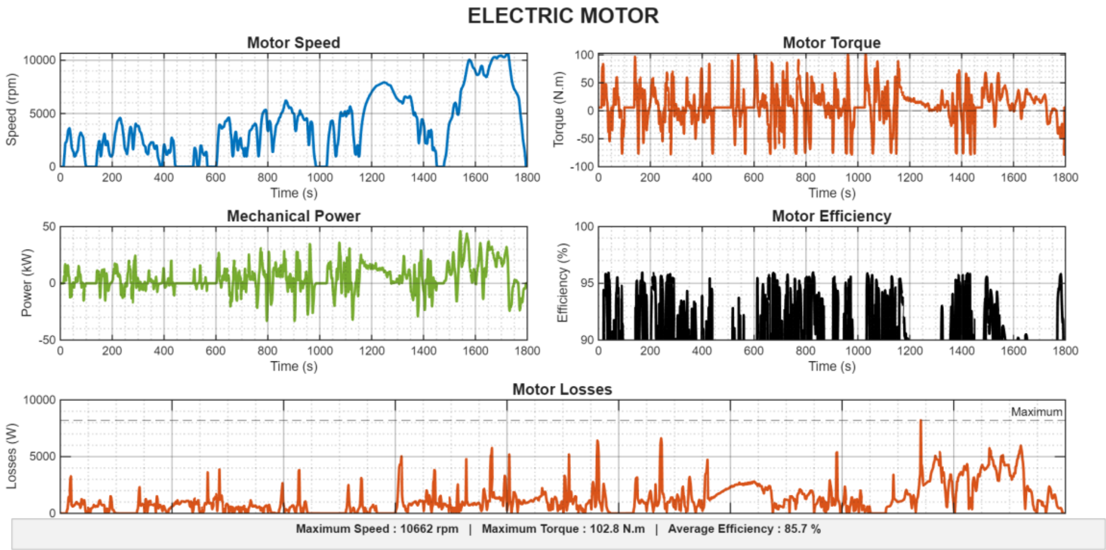

Figure 8: Electromechanical behavior of the PMSM throughout the WLTC Class 3b

Battery management system

Figure 9 illustrates the electrical behavior of the lithium-ion battery throughout the WLTC Class 3b driving cycle by presenting the evolution of the state of charge (SOC), terminal voltage, current, exchanged power, and Joule losses. The battery model is based on coulomb counting for SOC estimation and an equivalent electrical circuit incorporating the open-circuit voltage and internal resistance, enabling an accurate representation of the charge and discharge processes occurring during the driving cycle.

As shown in Figure 9, the battery plays a key role in compensating for rapid variations in power demand. The highest discharge currents occur during transient acceleration phases, when the dynamic response of the proton exchange membrane fuel cell (PEMFC) is insufficient to instantaneously supply the required power. Conversely, deceleration phases promote regenerative braking, allowing kinetic energy to be recovered and resulting in a gradual increase in the battery SOC. The strong agreement between the evolution of the SOC, terminal voltage, and net exchanged energy confirms the validity of the implemented battery model and demonstrates that the internal losses are accurately represented.

Furthermore, Figure 9 highlights the central role of the battery within the proposed Equivalent Consumption Minimization Strategy (ECMS). The battery power, calculated as the difference between the power demanded by the electric drivetrain and the power supplied by the PEMFC, enables rapid load fluctuations to be absorbed while satisfying both the power capability and SOC constraints. This complementary operation between the fuel cell and the battery ensures continuous power delivery to the traction system, enhances the overall energy management stability, reduces hydrogen consumption, and contributes to preserving both system performance and battery lifetime.

Journal of Information Systems Engineering and Management
2026, 11(3s)
e-ISSN: 2468-4376
https://www.jisem-journal.com/

Research Article

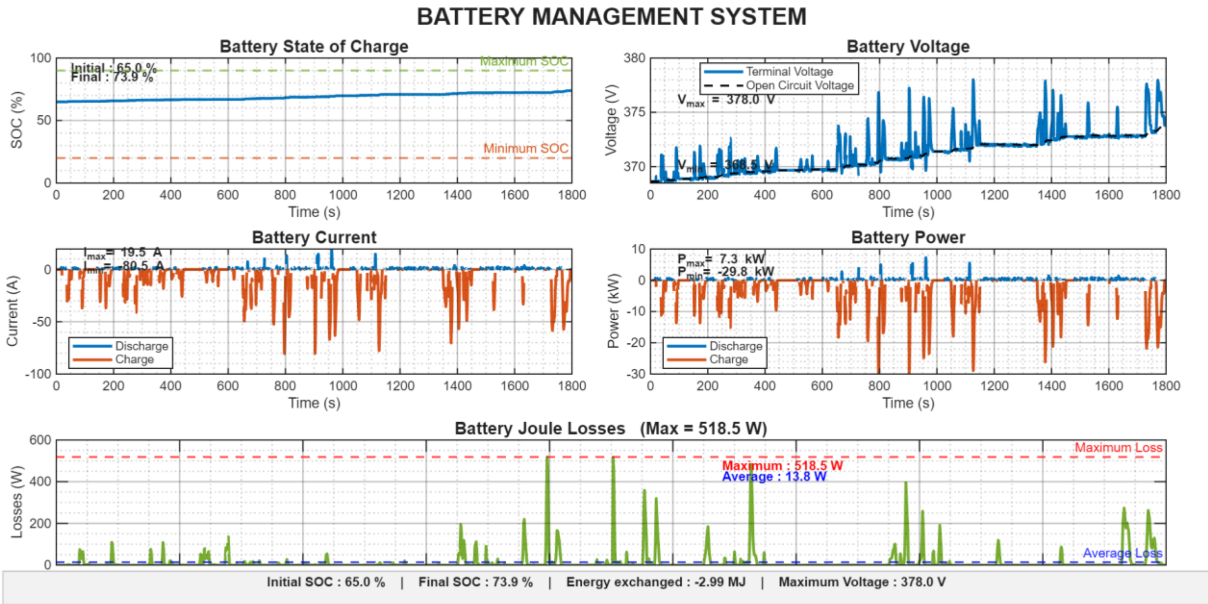

Figure 9: Battery Management System

PEM Fuel Cell System

Figure 10 presents the performance of the Proton Exchange Membrane Fuel Cell (PEMFC) throughout the WLTC Class 3b driving cycle by illustrating the evolution of the output power, stack current, instantaneous efficiency, and cumulative hydrogen consumption. The electrochemical model directly relates the delivered power to the hydrogen mass flow rate, while the fuel cell efficiency is described by a power-dependent efficiency map that accurately reproduces the behavior of a real PEMFC, with maximum efficiency achieved under partial-load operating conditions.

As shown in Figure 10, the fuel cell continuously adapts its operating point to the varying energy demand imposed by the WLTC driving cycle. Low power levels observed during urban driving alternate with higher power demands during high-speed operating conditions. The instantaneous efficiency varies between 40% and 60%, reflecting the different operating regions of the fuel cell. Incorporating this efficiency map provides a more realistic representation of the electrochemical system and reduces hydrogen consumption compared with a constant-efficiency model, while maintaining full consistency between the delivered electrical power and the corresponding hydrogen consumption.

Furthermore, Figure 10 highlights the crucial role of the fuel cell efficiency model within the proposed Equivalent Consumption Minimization Strategy (ECMS). The instantaneous hydrogen cost associated with each candidate power level is directly considered during the optimization process, enabling the controller to preferentially operate the fuel cell within its highest-efficiency regions. These results confirm the consistency of the developed electrochemical model and demonstrate that the predicted hydrogen consumption is fully consistent with the overall vehicle energy balance, thereby reinforcing the reliability and effectiveness of the proposed energy management strategy.

Journal of Information Systems Engineering and Management
2026, 11(3s)
e-ISSN: 2468-4376
https://www.jisem-journal.com/

Research Article

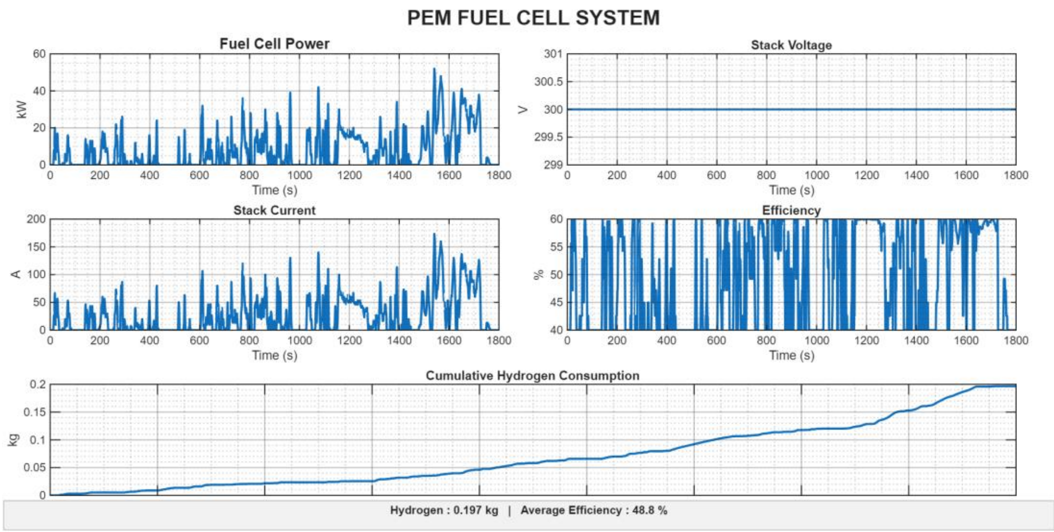

Figure 10: PEM Fuel Cell System

ECMS Energy Management

Figure 11 illustrates the operation of the implemented Equivalent Consumption Minimization Strategy (ECMS), which is responsible for the real-time power allocation between the Proton Exchange Membrane Fuel Cell (PEMFC) and the lithium-ion battery. At each simulation time step, the controller minimizes a cost function defined as the sum of the actual hydrogen consumption of the fuel cell and the equivalent hydrogen consumption associated with the battery power, weighted by an adaptive equivalence factor that depends on the battery state of charge (SOC). This optimization framework provides an effective trade-off between minimizing hydrogen consumption and maintaining the battery SOC within its desired operating range.

As shown in Figure 11, the proposed energy management strategy primarily relies on the fuel cell to satisfy the traction power demand under steady-state operating conditions, whereas the battery mainly supports rapid transient power demands and absorbs the energy recovered during regenerative braking. To more accurately reproduce the dynamic behavior of a real PEMFC system, a power ramp-rate limiter was incorporated into the model. This constraint captures the intrinsic dynamic response of the electrochemical system by automatically transferring rapid power fluctuations to the battery whenever the fuel cell cannot instantaneously follow the requested power. In addition, an SOC-based supervisory control layer was introduced to modify the operating mode when the battery reaches predefined upper or lower SOC thresholds, thereby improving the robustness of the energy management strategy under a wide range of operating conditions.

Furthermore, Figure 11 demonstrates the consistency between the ECMS controller and the underlying electrochemical fuel cell model. The cumulative hydrogen consumption estimated by the controller exactly matches that computed by the physical fuel cell model, confirming the consistency of the overall energy balance within the developed simulator. These results demonstrate that the proposed strategy achieves an efficient power distribution between the two energy sources while satisfying the dynamic constraints of the fuel cell and the operating limits of the battery, thereby providing a robust framework for the energy optimization of Fuel Cell Hybrid Electric Vehicles (FCHEVs).

Journal of Information Systems Engineering and Management
2026, 11(3s)
e-ISSN: 2468-4376
https://www.jisem-journal.com/

Research Article

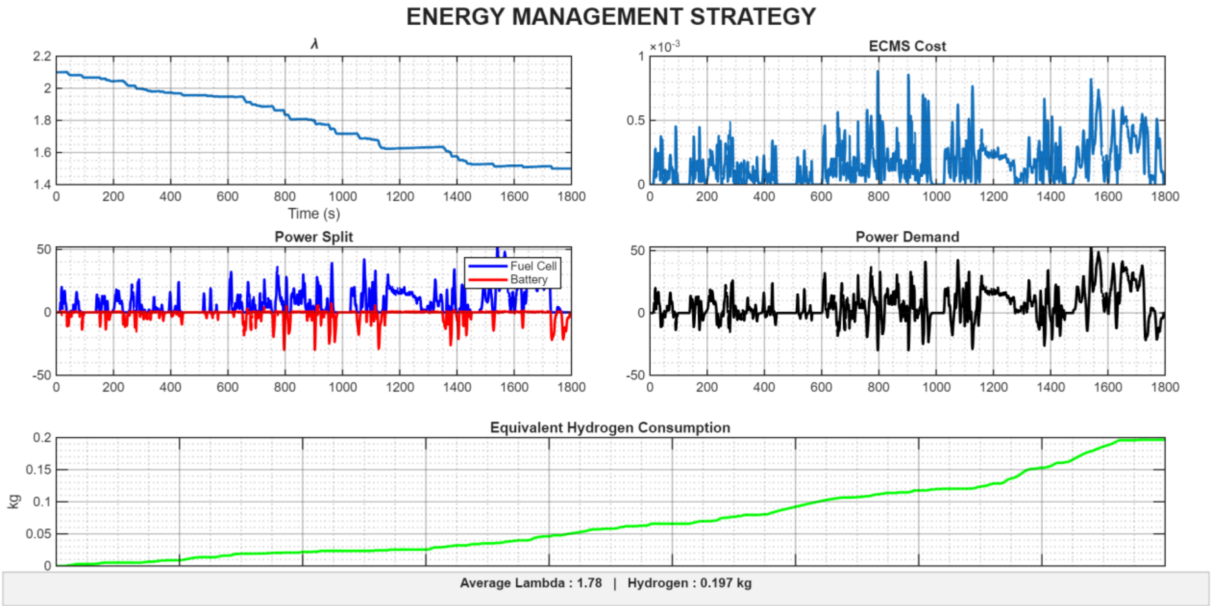

Figure 11: ECMS Energy Management

Caractérisation du moteur électrique

Figure 12 presents the electromechanical characterization of the Permanent Magnet Synchronous Motor (PMSM) employed in the Fuel Cell Hybrid Electric Vehicle (FCHEV). It includes the torque–speed characteristic, the power–speed curve, the motor efficiency map, and the projection of the operating points generated during the WLTC Class 3b driving cycle. This representation enables the actual operating conditions of the motor to be compared with its physical operating limits and provides a comprehensive assessment of the adequacy of its sizing for the intended application.

As illustrated in Figure 12, the PMSM exhibits the conventional operating characteristics of a permanent magnet synchronous machine, consisting of a constant-torque region followed by a constant-power region beyond the base speed. The operating points corresponding to the WLTC driving cycle are predominantly concentrated within the high-efficiency regions of the efficiency map, while the most demanding operating conditions remain well below the motor's maximum torque, power, and speed limits. Furthermore, the close agreement between the average efficiency derived from the efficiency map and that predicted by the dynamic motor model confirms the validity and internal consistency of the developed electromechanical model.

In addition, Figure 12 demonstrates that all power demands supplied to the proposed Equivalent Consumption Minimization Strategy (ECMS) remain within the operational envelope of the electric motor, ensuring saturation-free operation throughout the entire WLTC driving cycle. These results confirm that the selected PMSM is appropriately sized for the FCHEV powertrain and is capable of meeting the vehicle's dynamic performance requirements while maintaining a high level of energy efficiency under all driving conditions considered.

Journal of Information Systems Engineering and Management
2026, 11(3s)
e-ISSN: 2468-4376
https://www.jisem-journal.com/

Research Article

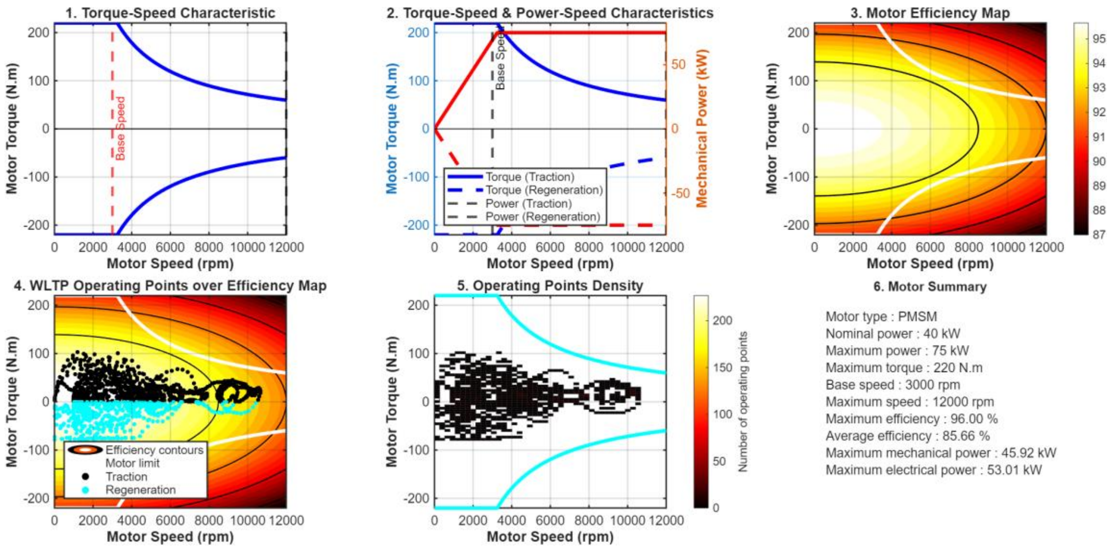

Figure 12: Electromechanical characterization of the PMSM used in FCHEV

Validation of the SOC Threshold-Based Switching Logic

Figure 13 presents the validation of the state-of-charge (SOC) threshold-based switching logic incorporated into the proposed energy management strategy. Two extreme operating scenarios are considered to explicitly activate both supervisory control modes: the first with an initial SOC of 85%, above the upper threshold, and the second with an initial SOC of 35%, below the lower threshold. These simulations, performed over the WLTC Class 3b driving cycle, enable the behavior of the supervisory controller to be evaluated under operating conditions that do not occur during the reference simulation.

As illustrated in Figure 13, when the initial SOC exceeds the upper threshold, the control strategy prioritizes battery utilization to gradually reduce the SOC toward its nominal operating range, while temporarily decreasing the contribution of the Proton Exchange Membrane Fuel Cell (PEMFC). Conversely, when the initial SOC falls below the lower threshold, the fuel cell delivers power exceeding the traction demand to actively recharge the battery until the SOC returns to the prescribed operating range. Once the SOC re-enters the admissible region, the controller automatically resumes the standard Equivalent Consumption Minimization Strategy (ECMS), ensuring a smooth and continuous transition between the different operating modes.

These results confirm the correct operation of the proposed supervisory control logic and demonstrate its ability to maintain the battery SOC within the desired operating range without disrupting the power distribution between the fuel cell and the battery. The successful validation of these boundary-case scenarios further demonstrates the robustness of the developed energy management algorithm and its capability to handle extreme initial operating conditions while preserving the overall consistency of the vehicle energy balance.

Journal of Information Systems Engineering and Management
2026, 11(3s)
e-ISSN: 2468-4376
https://www.jisem-journal.com/ Research Article

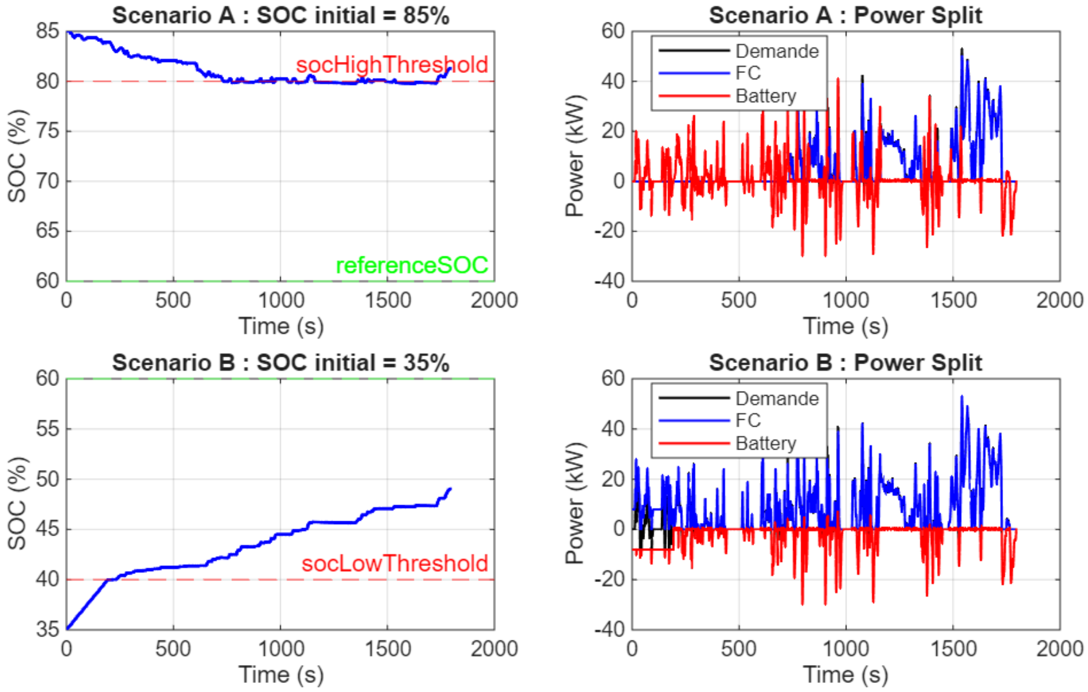

Figure 13. Validation of the SOC Threshold-Based Switching Logic

General Discussion and Overall Assessment

The results presented in Figures 6–13 provide a comprehensive and physically consistent representation of the behavior of the proposed Fuel Cell Hybrid Electric Vehicle (FCHEV) under the WLTC Class 3b driving cycle. Several independent cross-validations confirm the reliability of the developed simulation framework. These include the consistency between the motor torque and the wheel torque through the transmission gear ratio, the excellent agreement between the average motor efficiencies obtained from the dynamic model and the efficiency map, the consistency between the battery state-of-charge (SOC) variation and the corresponding energy balance, and the identical cumulative hydrogen consumption predicted by both the electrochemical fuel cell model and the Equivalent Consumption Minimization Strategy (ECMS). Together, these results demonstrate the internal consistency and physical validity of the proposed modeling approach.

One of the most significant findings of this study is the energy management behavior achieved with the adopted ECMS calibration. Under the selected equivalence factor settings, the Proton Exchange Membrane Fuel Cell (PEMFC) acts as the primary energy source during steady-state operation, whereas the lithium-ion battery fulfills a complementary role by recovering regenerative braking energy and providing transient power assistance whenever the fuel cell is unable to satisfy rapid power variations because of its dynamic response limitations. This operating behavior results directly from the selected adaptive equivalence factor and is fully consistent with the theoretical formulation of the proposed energy management strategy.

The developed simulator also incorporates several improvements over previous versions. In particular, the fuel cell is modeled using a realistic power-dependent efficiency map rather than a constant efficiency, and its transient behavior is represented through a power ramp-rate limitation, resulting in a more accurate description of the electrochemical system. Although further refinements remain possible—such as extending the visualization of the motor efficiency map to include low-load operating regions—the proposed simulation framework provides a robust and physically consistent platform for analyzing FCHEV energy management strategies. Moreover, the additional validation performed under extreme initial SOC conditions confirms the correct operation of the proposed SOC threshold-based supervisory control, further strengthening the reliability of the overall energy management architecture.

Journal of Information Systems Engineering and Management
2026, 11(3s)
e-ISSN: 2468-4376
https://www.jisem-journal.com/

Research Article

CONCLUSION

This paper presented the development and validation of a comprehensive MATLAB-based simulator for a Fuel Cell Hybrid Electric Vehicle (FCHEV) integrating an Equivalent Consumption Minimization Strategy (ECMS) for real-time energy management. The proposed modular architecture combines detailed multiphysics models of the vehicle powertrain with an enhanced ECMS algorithm incorporating fuel cell power gradient limitation and battery state-of-charge supervision. Simulation results obtained over the WLTC Class 3b driving cycle demonstrated the numerical robustness and physical consistency of the developed platform through systematic cross-validation of energy flows, battery behavior, and hydrogen consumption. The proposed simulator accurately reproduces the power-sharing mechanism between the fuel cell and the battery while providing a reliable framework for evaluating FCHEV energy management strategies. Owing to its modular design, the platform can be readily extended to incorporate higher-fidelity component models, adaptive ECMS formulations, predictive control approaches, and artificial intelligence-based energy management algorithms for future research.

REFRENCES

[1] X. Yue et al., "Energy management strategies for fuel cell hybrid electric vehicles: Classification, comparison, and outlook," Energy Conversion and Management, vol. 270, 116179, 2022.

[2] M. Rasool, M. A. Khan, and R. Zou, "A Comprehensive Analysis of Online and Offline Energy Management Approaches for Optimal Performance of Fuel Cell Hybrid Electric Vehicles," Energies, vol. 16, no. 8, 2023.

[3] J. E. Dakurah, H. Solmaz, and T. Kocakulak, "Modeling of a PEM Fuel Cell Electric Bus with MATLAB/Simulink," Automotive Experiences, vol. 7, no. 2, 2024.

[4] M. Diana et al., "A MATLAB script and a methodology for the powertrain design of a fuel cells-battery hybrid electric supercar," Energy Conversion and Management: X, vol. 23, 2024.

[5] C. Steindl and P. Hofmann, "Systematic Development Approach for a Hybrid Electric Powertrain Using Fuel-Cell-in-the-Loop Test Methodology," SAE Technical Paper, 2023.

[6] X. Lü et al., "Adaptive energy management strategy for FCHEV based on improved proximal policy optimization in deep reinforcement learning algorithm," Energy Conversion and Management, 2024.

[7] W. Sun et al., "Research on ECMS Based on Segmented Path Braking Energy Recovery in a Fuel Cell Vehicle," Energy Engineering, vol. 121, no. 1, 2024.

[8] "MLD Modeling and MPC-Based Energy Management Strategy for Hydrogen Fuel Cell/Supercapacitor Hybrid Electric Vehicles," World Electric Vehicle Journal, vol. 15, 2024.

[9] "Advanced Equivalent Consumption Minimization Strategy for Fuel Cell Hybrid Electric Vehicles," Journal of Cleaner Production, vol. 437, 140366, 2024.

[10] C. Du et al., "Degradation-considering adaptive equivalent consumption minimization strategy for fuel cell electric vehicles," Proceedings of the Institution of Mechanical Engineers, Part D, 2025.

[11] X. Lü et al., "Adaptive energy management strategy for FCHEV based on improved proximal policy optimization in deep reinforcement learning algorithm," Energy Conversion and Management, 2024.

[12] P. Pramod Muthyala et al., "Comparative study of real-time A-ECMS and rule-based energy management strategies," Energy Conversion and Management: X, 2024.

[13] X. Yue et al., "Energy management strategies for fuel cell hybrid electric vehicles: Classification, comparison, and outlook," Energy Conversion and Management, 2022.

[14] Khalatbarisoltani, H. Zhou, X. Tang, M. Kandidayeni, L. Boulon, and X. Hu, "Energy Management Strategies for Fuel Cell Vehicles: A Comprehensive Review of the Latest Progress in Modeling, Strategies, and Future Prospects," IEEE Transactions on Intelligent Transportation Systems, vol. 25, no. 1, pp. 14–32, 2024.

[15] H. Wang, A. Gaillard, Z. Li, R. Roche, and D. Hissel, "Multiple-Fuel Cell Module Architecture Investigation: A Key to High Efficiency in Heavy-Duty Electric Transportation," IEEE Vehicular Technology Magazine, vol. 17, no. 3, pp. 94–103, 2022.

[16] Y. Shen, J. Xie, T. He, L. Yao, and Y. Xiao, "CEEMD-Fuzzy Control Energy Management of Hybrid Energy Storage Systems in Electric Vehicles," IEEE Transactions on Energy Conversion, vol. 39, no. 1, pp. 555–566, 2024.

A. Khalatbarisoltani, L. Boulon, and X. Hu, "Integrating Model Predictive Control With Federated Reinforcement Learning for Decentralized Energy Management of Fuel Cell Vehicles," IEEE Transactions on Intelligent Transportation Systems, vol. 24, no. 12, pp. 13639–13653, 2023.

[17] S. Yang, J. Wang, F. Zhang, and J. Xi, "Self-Adaptive Equivalent Consumption Minimization Strategy for Hybrid Electric Vehicles," IEEE Transactions on Vehicular Technology, vol. 70, no. 1, pp. 189–202, 2021.

A. Sciarretta, M. Back, and L. Guzzella, “Optimal control of parallel hybrid electric vehicles,” IEEE Transactions on Control Systems Technology, vol. 12, no. 3, pp. 352–363, 2004.

B. C. Chan, “The state of the art of electric, hybrid, and fuel cell vehicles,” Proceedings of the IEEE, vol. 95, no. 4, pp. 704–718, 2007.

[18] J. Wang, T. Shen, and S. Chen, “Modeling and control of permanent magnet synchronous motors for electric vehicle applications,” IEEE Transactions on Transportation Electrification, vol. 8, no. 2, pp. 1345–1358, 2022.

[19] M. Morimoto, S. Ooi, and Y. Takeda, “High-performance control of PMSM drives for EV applications: A review,” IEEE Transactions on Industrial Electronics, vol. 69, no. 5, pp. 4512–4525, 2023.

[20] Kada Hartani, Abdelkader Merah, Azeddine Draou, " Stability Enhancement of Four-in-Wheel Motor-Driven Electric Vehicles Using an Electric Differential System ", Journal of Power Electronics, Vol. 15, N°5, pp. 1244-1255, 2015, ISSN 1598-2092.

[21] S. Piller, M. Perrin, and A. Jossen, “Methods for state-of-charge determination and their applications,” Journal of Power Sources, vol. 96, no. 1, pp. 113–120, 2001.

[22] J. Jaguemont, L. Boulon, and Y. Dubé, “A comprehensive review of lithium-ion batteries used in hybrid and electric vehicles,” Renewable and Sustainable Energy Reviews, vol. 44, pp. 663–686, 2015.

[23] G. L. Plett, “Extended Kalman filtering for battery management systems of LiPB-based HEV battery packs,” Journal of Power Sources, vol. 134, no. 2, pp. 252–261, 2004.

[24] M. Dubarry and B. Y. Liaw, “Identify capacity fading mechanism in a commercial Li-ion battery,” Journal of Power Sources, vol. 194, no. 1, pp. 541–549, 2009.

[25] J. Larminie and A. Dicks, Fuel Cell Systems Explained, 2nd ed., Wiley, 2003.

[26] R. O’Hayre, S.-W. Cha, W. Colella, and F. B. Prinz, Fuel Cell Fundamentals, 3rd ed., Wiley, 2016.

A. Brouwer, “Dynamic modeling of proton exchange membrane fuel cells,” Journal of Power Sources, vol. 162, no. 1, pp. 436–446, 2006.

[27] J. Wu, X. Wang, and S. Li, “Review on PEM fuel cell modeling for transportation applications,” Applied Energy, vol. 255, 2019.

[28] J. Larminie and A. Dicks, Fuel Cell Systems Explained, 2nd ed., Wiley, 2003.

[29] R. O’Hayre, S.-W. Cha, W. Colella, and F. B. Prinz, Fuel Cell Fundamentals, 3rd ed., Wiley, 2016.

A. Brouwer, “Dynamic modeling of proton exchange membrane fuel cells,” Journal of Power Sources, vol. 162, no. 1, pp. 436–446, 2006.

Journal of Information Systems Engineering and Management
2026, 11(3s)
e-ISSN: 2468-4376
https://www.jisem-journal.com/

Research Article

[30] J. Wu, X. Wang, and S. Li, "Review on PEM fuel cell modeling for transportation applications," Applied Energy, vol. 255, 2019.

[31] F. Z. Peng, "Z-source inverter," IEEE Transactions on Industry Applications, vol. 39, no. 2, pp. 504–510, 2003.

[32] R. W. Erickson and D. Maksimović, Fundamentals of Power Electronics, 2nd ed., Springer, 2001.

[33] L. Serrao, S. Onori, and G. Rizzoni, "ECMS as a real-time optimal control approach for hybrid electric vehicles," IEEE Transactions on Control Systems Technology, vol. 19, no. 6, pp. 1620–1631, 2011.

A. Sciarretta and L. Guzzella, "Control of hybrid electric vehicles," IEEE Control Systems Magazine, vol. 27, no. 2, pp. 60–70, 2007.

[34] S. E. Li, K. Li, and R. G. Song, "Energy management strategies for hybrid electric vehicles: A review," Applied Energy, vol. 172, pp. 280–293, 2016.

LIST OF SYMBOLS

F_{tr}: traction force developed at the wheels (N) ;

F_{roll}: rolling resistance (N) ;

F_{aero}: aerodynamic resistance (N) ;

F_{grade}: resistance due to the road grade (N) ;

F_{acc}: inertial force (N).

C_{rr}: rolling resistance coefficient (dimensionless).

F_{aero}: aerodynamic drag force (N) ;

ρ: air density ($\mathrm{kg/m^3}$);

C_d: aerodynamic drag coefficient (dimensionless) ;

A_f: frontal area of the vehicle ($\mathrm{m^2}$);

v: relative velocity of the vehicle with respect to the air ($\mathrm{m/s}$).

F_{grade}: force due to the road grade (N) ;

θ: road angle (rad).

F_{acc}: inertial force (N) ;

m: total mass of the vehicle (kg) ;

a: longitudinal acceleration ($\mathrm{m/s^2}$).

J: total moment of inertia of the rotating parts ($\mathrm{kg \cdot m^2}$);

ω_m: mechanical angular speed of the rotor ($\mathrm{rad/s}$) ;

T_e : electromagnetic torque ;

T_L : load torque ;

T_f : friction torque.

V_{min}: voltage corresponding to the minimum SOC ;

V_{max}: voltage corresponding to a fully charged battery.

V_{cell}: actual cell voltage (V) ;

Journal of Information Systems Engineering and Management
2026, 11(3s)
e-ISSN: 2468-4376
https://www.jisem-journal.com/
Research Article

E_N: reversible voltage given by the Nernst equation (V) ;

η_{act}: activation overvoltage (V) ;

η_{ohm}: ohmic overvoltage (V) ;

η_{conc}: concentration overvoltage (V).

V_{stack} : the total stack voltage (V) ;

N_{cell} : the number of cells.

V_{stack} : the stack voltage (V) ;

N_{cell} : the number of cells ;

V_{cell} : the voltage of an individual cell (V).

P_{FC} : the electric power (W) ;

I_{FC} : the current supplied by the stack (A).

$\dot{n}_{H_2}$: the molar flow rate of hydrogen (mol·s $^{-1}$) ;

I_{FC} : the stack current (A).

F : the Faraday constant.

N_{cell} : the number of cells in the stack.

m_{H_2}The total mass consumed P_{FC} is the electric power delivered ;

$\dot{m}_{H_2}$: the mass flow rate of hydrogen ;

PCI_{H_2} : the lower heating value.

i_L : the current in the inductor (A) ;

V_{dc} : the DC bus voltage (V).

v_L : the voltage across the inductor (V) ;

L : the inductance (H).

i_C :the capacitor current ;

C : the filtering capacitance.

V_{FC} : the fuel cell voltage ;

D : the duty cycle.

i_{load} : the current drawn by the traction inverter.

V_{bat} : the battery voltage.

t_{on} : the switch conduction time ;

T_s : the switching period.

P_{mag} : the magnetic losses ;

P_{aux} : the auxiliary losses.

P_{FC} : the power produced by the fuel cell ;

P_{dc} is the power available on the DC bus.

Journal of Information Systems Engineering and Management
2026, 11(3s)
e-ISSN: 2468-4376
https://www.jisem-journal.com/

Research Article

P_{dem} : the power demanded by the electric motor ;

P_{FC} : the power delivered by the fuel cell ;

P_{bat} : the power supplied or absorbed by the battery.

SOC_{min} : the minimum allowable limit ;

SOC_{max} : the maximum limit.

P_{FC}^{min} : avoids operation at very low, inefficient load ;

P_{FC}^{max} : the rated power of the stack.

I_{bat} : the battery current ;

Q_{nom} is its rated capacity.

$\dot{m}_{eq}$ is the total equivalent hydrogen consumption (kg·s $^{-1}$) ;

$\dot{m}_{H_2}$ is the actual consumption of the fuel cell ;

$\dot{m}_{bat}^{eq}$ is the equivalent consumption associated with the battery.

P_{FC} is the power delivered by the fuel cell (W) ;

η_{FC} is its instantaneous efficiency ;

PCI_{H_2} is the lower heating value of hydrogen (J·kg $^{-1}$).

s is the equivalence factor (dimensionless).

η_{dis} is the discharge efficiency.

η_{ch} is the charge efficiency.

η_{bat} represents the appropriate efficiency (charging or discharging).